Iraqi National Journal of Earth Science

www.earth.uomosul.edu.iq

Overpressure and Under-Compaction Mechanism Effect on Pore and Fracture Pressure Development of Mauddud Formation, Badra Oil Field, Eastern Iraq

Mohammed Almojahed Farooq Abdalla [1*], Nagham Jasim Al-Ameri [2]

[1,2] Petroleum Engineering Department, College of Engineering, University of Baghdad, Baghdad, Iraq.

Article information

Received: 01- Nov-2024

Revised: 30- Nov -2024

Accepted: 20- Dec -2024

Available online: 01- Jan -2026

Keywords:
Compaction Mechanism,
Overburden Pressure,
Pore Pressure,
Fracture Pressure,
Microfacies analysis,

Correspondence:
Name: Mohammed Almojahed Farooq Abdalla

Email: muhammed.farooq2208m@coeng.uobaghdad.edu.iq

ABSTRACT

Accurate pore and fracture pressure detection is a major step in successful drilling operations design. The overestimation of these parameters absolutely leads to serious problems throughout and after well drilling. This study is concerned with the characterization and analysis of the most significant diagenetic processes that degrade or improve the reservoir characteristics of the Mauddud Formation in the Badra oil field. The primary goal of this research is to estimate the pore pressure and fracture pressure using well logging data by Techlog 2015 software in order to assess the impact on the estimation of the mud weight window (MWW). The estimated values of formation pressures are then analyzed according to different diagenetic processes affecting the reservoir under study. These important reasons, such as sedimentary texture and original structure, have been analyzed in this study based on the images of both Scanning Electron Microscopy (SEM) and thin section (TS) of many samples taken at different depths of the studied reservoir to cover the vertical changes of the formation. The results show that the value of the safe mud weight window must range from 2.3 to 3.4 ppg, and it becomes narrower and more dangerous when the wells cross the edge of the anticline structure of the reservoir.

DOI: 10.33899/injes.v26i1.60209,

تأثير آلية الضغط الزائد ونقص الضغط على تطور ضغط المسام والكسر في تكوين مودود، حقل بدرة النفطي، شرق العراق

محمد المجاهد عبدالله [1*] ، نغم جاسم [2]

[2,1] قسم هندسة النفط، كلية الهندسة، جامعة بغداد، بغداد، العراق.

معلومات الارشفة

تاريخ الاستلام: 01- نوفمبر- 2024

تاريخ المراجعة: 30- نوفمبر- 2024

تاريخ القبول: 20- ديسمبر- 2024

تاريخ النشر الالكتروني: 01- يناير- 2026

الكلمات المفتاحية:

آلية الضغط،

الضغط الزائد،

ضغط المسام،

ضغط الكسر،

تحليل السحنات الدقيقة،

المراسلة:

الاسم: محمد المجاهد عبدالله

Email: muhammed.farooq2208m@coeng.uobaghdad.edu.iq

الملخص

يعد الكشف الدقيق عن ضغط المسام والكسر خطوة رئيسة في تصميم عمليات الحفر الناجحة. إن المبالغة في تقدير هذه المتغيرات تؤدي بالتأكيد إلى مشاكل خطيرة أثناء حفر الآبار وبعدها. تهتم هذه الدراسة بتوصيف وتحليل أهم العمليات التحويرية التي تؤدي إلى تحلل أو تحسين الخصائص المكمنية لتكوين مودود في حقل بدرة النفطي. الهدف الأساس من هذا البحث هو تقدير ضغط المسام وضغط الكسر باستخدام بيانات تسجيل الآبار بواسطة برنامج (Techlog 2015) من أجل تقييم التأثير على تقدير نافذة وزن الطين (MWW). ومن ثم تم تحليل القيم المقدرة لضغوط التكوين وفقا لتأثيرات العمليات التحويرية المختلفة على المكمن قيد الدراسة. تم تحليل هذه الأسباب المهمة مثل النسيج الرسوبي والبنية الأصلية في هذه الدراسة بناءً على صور كل من المجهر الإلكتروني الماسح (SEM) والشرائح الصخرية الرقيقة (TS) للعديد من العينات المأخوذة من أعماق مختلفة من المكمن المدروس لتغطية التغييرات الرأسية للتكوين. وتبين النتائج أن قيمة نافذة وزن الطين الآمن (MWW) يجب أن تتراوح مابين 2.3 إلى 3.4 باوند لكل غالون، وتصبح هذه القيمة ضيقة وأكثر خطورة عندما تقترب الآبار من حافة هيكل طية التكوين.

DOI: 10.33899/injes.v26i1.60209,

Introduction

At a certain depth in a studied formation, the stress that actually affects is made up of vertical stress, maximum horizontal stress, and minimum horizontal stress. Pore pressure is the force that acts on liquids inside the pores of rocks. Pore pressure is an important part of the mechanical factors used in the drilling plan and geological and geomechanical studies to determine the horizontal stresses (Rasouli et al., 2011; Bandara and Al-Ameri, 2024). According to Aadnoy and Looyeh (2011). The rocks are porous materials with a rocky matrix and liquid. Not all formation stresses are carried by the rock matrix; some are carried by the fluids in the rock's pores (Aman et al., 2018). Hence, the effective stress is the percentage of stress that the rock matrix bears.

The diacritical pore pressure in shale formation may be determined using sonic and resistivity logs, as stated by Rasouli et al. (2011). Pore pressure is classified into three classes according to its magnitude, as mentioned by Zhang (2013), as follows: first, the normal pore pressure, which is the pressure generated by the fluid column from the formation's surface to the bottom. It varies due to the kind of fluid, temperature gradient, gases present, and dissolved solids content; therefore, it is not constant. Second, the abnormal pore pressure, which refers to pore pressure greater than the hydrostatic pressure of the formation. Abnormal pressure is

assumed to be caused by extranormal hydrostatic or increased pressure. Third, the subnormal pore pressure, in which the formation pressure for the stated depth is lower than the hydrostatic fluid pressure.

There are two methods for determining pore pressure (direct and indirect). In permeable formations, methods like Drill Stem Testing (DST), Repeated Formation Testing (RFT), and Modular Dynamic Formation Tester (MDT) can be used to determine the normal pore pressure of the formation (Najibi et al., 2005).

To estimate pore pressure from logs, geophysical measurement is used. This method is commonly used because the direct methods are costly, risky, time-consuming, and provide poor measurements in some intervals. Furthermore, direct methods cannot quantify pore pressure in shale (impermeable zone) or clay rocks (Aadnoy and Ong, 2003). Therefore, the geophysical measurement provides a continuous pore pressure profile along the interval of interest. To minimize suspicion, the determined pore pressure can be matched with the point of formation pressure, which is measured by a direct method, and then the profile is calibrated for direct pressure measurements to minimize suspicion in the determined pore pressure.

Formation breakdown pressure, as mentioned by Chen (2017), or fracture pressure, as mentioned by Aadnoy and Looyeh (2011), is required to cause rock fracture at a depth. The fracture pressure may be less than the minimum horizontal stress if the rocks already have pre-existing flaws (Chen, 2017). The maximum fracture pressure for unaffected rocks will occur following the initiation of a tensile failure and the occurrence of mud loss. When the tensile strength and the least hoop stress are equivalent, the fracture pressure can be determined using Kirsch's solution (Haimson and Fairhurst, 1969).

In the current study, four wells (A, B, C, and D), which are dispersed along the Badra oil field anticline structure, have been used to investigate different formation pressures, including overburden, pore, and fracture pressure, to estimate the safe mud weight window.

Geological Background

One of the major carbonate reservoirs found in the Arabian Plate region is present in the Mauddud Formation (Cross et al., 2010). Across the Arabian plate, the formation is thick and has a regional distribution (Sadooni and Alsharhan, 2003). Oil is produced from limestone units in the Badra oil field in eastern Iraq by the Mauddud Formation (Faisal and Mahdi, 2020b). Limestone with a thin coating of dolomite, stylolitic dolomite, and detrital and chalky limestone make up the Mauddud Formation in the Badra oil field. A wealth of fossils supports an Albian age. Initially, it was believed that the formation continued into the Cenomanian due to the frequent appearance of certain Orbitolina concave group species; the formation was deposited in a neritic, occasionally shoal environment (Ghafor et al., 2023).

The Mauddud Formation has a conformable and gradational lower contact with Nahr Umr, Lower Balambo, and Lower Sarmord formations. The top contact is characterized by a break and is either nonsequential or unconformable; it represents an unconformity in north central-, northern-, and northeastern Iraq (Jassim and Goff, 2006).

The Badra field is situated in eastern Iraq, as shown in Fig. 1A, close to the borders between Iraq and Iran. It lies between the Mesopotamian Zone (Tigris subzone) and the Foothill Zone (Himreen-Makhul subzone). The Mesopotamian zone is the easternmost unit of the Stable Shelf. The zone likely underwent uplift during the Hercynian deformation, but it declined in the Late Permian period. Beneath the Quaternary cover, the zone is made up of buried faulted structures that are divided by wide synclines. As illustrated in Fig. 1B, some NE-SW trending fold structures exist; in the eastern part of the zone, the fold structures mainly go NW-SE, while in the southern part, they trend N-S. (Jassim and Goff, 2006). The Tigris, Euphrates, and Zubair subzones are the three subzones that make up the Mesopotamian Zone.

The largest and most mobile Mesopotamian Zone unit is the Tigris Subzone. Long normal faults go alongside broad synclines and small anticlines that trend NW-SE. The zone has an EW transversal trend and two sets of low-amplitude, NW-SE trending buried anticlines linked to longitudinal faults (Faisal and Mahdi, 2020a).

This portion of the Unstable Shelf is called the Foothill Zone. The zone contains extremely thick Miocene-Pliocene molasses sediments (3 km thick) and the lowest Precambrian basement in Iraq (13 kilometers). The zone's two longitudinal components are the Makhul-Hemrin Subzone in the southwest and the Subzone Butmah-Chemhemal in the northeast. The Foothill Zone's structurally deepest area is the Makhul-Hemrin Subzone. Long, conspicuous NW-SE or E-W trending anticlines with decollement thrust faults make up the Subzone. The Subzone's anticlines extend more than 100 kilometers (Jassim and Goff, 2006). The Badra field structure is an asymmetrical NW-SE anticline trending, with a more gradual NE flank and a sharply descending SW flank (Kareem, 2020).

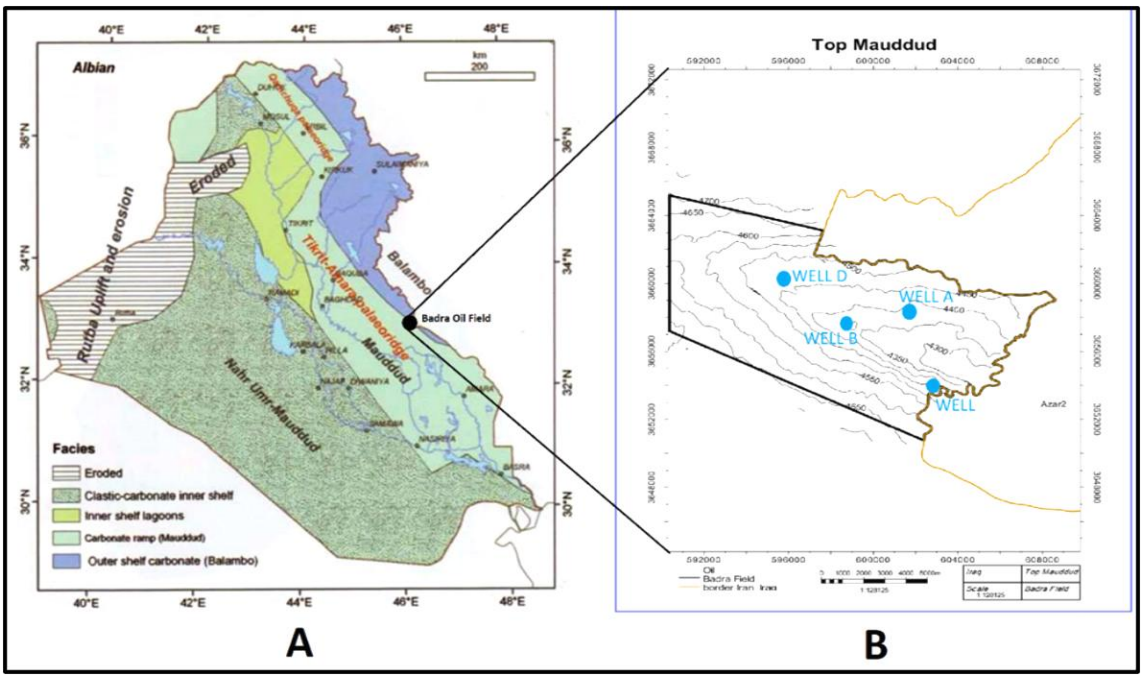

Fig. 1. A. Iraqi geological map (Jassim and Goff, 2006), B. Top Mauddud formation (Kareem, 2020).

Diagenesis Processes in Mauddud Formation

The physical, chemical, and biological processes that result in alterations, such as compaction, cementation, recrystallization, and others, are referred to as diagenesis. Diagenetic processes have significance for several reasons. They have the power to alter the content and texture of sediment significantly, and in some cases, they can even destroy the original structures. The porosity and permeability characteristics of sediment, which regulate the sediment's ability as a reservoir for water, gas, or oil, are likewise impacted by diagenesis. The above processes might be involved in generating or obstructing porosity. The Mauddud Formation has processes including neomorphism, dissolution at some points, cementation, micritization, compaction, and dolomitization. An overview of these procedures is seen below:

Micritization

It is the most frequent process that affects the skeletal pieces in the Mauddud Formation's bioclastic packstones and bioclastic wackestone microfacies. Blue-green algae or fungus significantly affects the micritization process in a stagnant marine phreatic zone. Micritization is an early diagnostic process that mostly affects benthonic foraminifera, particularly Orbitolinids and Miliolids. It is highly prevalent in the facies of the Mauddud Formation (Al-Dabbas et al., 2010).

Cementation

An essential diagnostic process minimizes pores by filling the space created by cement between the main and/or secondary porosity (Longman, 1980). The Mauddud Formation contains calcite cement. It completely or partially obstructs pores. The Mauddud Formation has been found to include the following forms of calcite cement:

a) Drusy Cement

The production of drusy mosaic cement is distinguished by calcite crystals that fill pore spaces, whose size increases toward the center of interparticle voids or pores (Flügel and Munnecke, 2010). Anhedral and subhedral crystals, which fill the moldic porosity, are characteristic of the cement type mentioned above. This cement's properties suggest a quick cementing process (Longman, 1980). It is widespread in the Mauddud Formation's microfacies and significantly decreases the secondary porosity, as shown in Fig. 2 (Sample A).

b) Granular -Blocky- Cement

Blocky cement is created in the later stages of diagenesis processes, frequently after sediments have been exposed to pressure from the ocean and lithified. Transparency and anhedral or subhedral calcite crystals with sizes ranging from 10 to 60 mm are characteristics of blocky cement (Flügel, 2012). The high crystal sizes in saturated solution indicate slow crystallization speeds (Flügel and Munnecke, 2010). The Mauddud Formation's mud and grain-supported microfacies include these huge cement crystals, as shown in Fig. 2 (Sample B).

c) Syntaxial Rim Cement

Within the microfacies of the Mauddud Formation, syntaxial rim cement is formed when crystals grow around echinoderm plate fragments to form optically continuous crystals. These crystals have an early diagenetic origin and are formed of either aragonite or calcite. This suggests the early formation of freshwater phreatic cement (Flügel and Munnecke, 2010). This kind of cement decreases the porosity between particles, especially in grain-supported microfacies, as shown in Fig. 2 (Sample C).

Neomorphism

A term first used by Folk (1965) to describe escalating neomorphism is the process by which a few giant crystals grow into and replace the micritic matrix, converting tiny crystals to massive ones (Scholle and Ulmer-Scholle, 2005). Both micrite and fossils from the microfacies undergo recrystallization. When skeletal grains recrystallize, they lose their original structure. Microspar or pseudospar is a neomorph of micrite. The degree of preservation demonstrates that neither micrite nor neomorphic skeletal grains developed a significant porosity.

Dissolution

The primary diagenetic process that enhances the porosity and permeability of the Mauddud Formation is dissolution. This appears to be affected by the solubility of minerals. For example, calcium carbonate is more soluble when transitioning from aragonite and high-magnesium to low-magnesium calcite. Different types of pores, such as moldic and vuggy ones, are created by dissolution (Choquette and Pray, 1970). These varieties, which range in size as shown in Fig. 3 (Sample C), were discovered in the Mauddud Formation. The widespread vugs and molds in the Mauddud Formation are evidence of significant disintegration occurrences. Certain skeletal grains, like echinoderms, are neither dissolved nor dolomitized and are composed of magnesium calcite (Enos, 1988).

Dolomitization

Dolomitization is transforming lime mud, either wholly or partially, into dolomite by substituting magnesium carbonate ($MgCO_3$) for $CaCO_3$ by the action of magnesium-containing water (Flügel and Munnecke, 2010). Dolomitization is even more widespread in mud-

dominated microfacies in the Mauddud Formation, where skeleton grain fragments from the original microfacies can still be seen, as shown in Fig. 2 (Samples F and E).

Compaction

Compaction causes the thickness of the overlying sediments to decrease, which lowers porosity and rock volume. There are two compaction-process categories (mechanical and chemical) (Croizé, 2010). Soon after deposition, mechanical compaction may start, resulting in micrite envelopes' collapse, elongated bioclasts' flattening toward the bedding plane, and tighter packing of grains. Stylolite, created by mixing dissolution and compaction, and in all carbonate rock textures, is a chemical compaction symbol. Pressure solution produced Stylolites, which result from the solution around grain contact sites that react to pressure as shown in Fig. 2 (Sample D).

Fracturing

In carbonate rocks, fractures are often significant secondary structures that arise from either compaction or the local tectonic regime (Flügel, 2012). Fracture has a small effect on the Mauddud Formation and is mostly observed in the rudistid facies. They can be filled with calcite cement, as shown in Fig. 3 (Sample D), or left open.

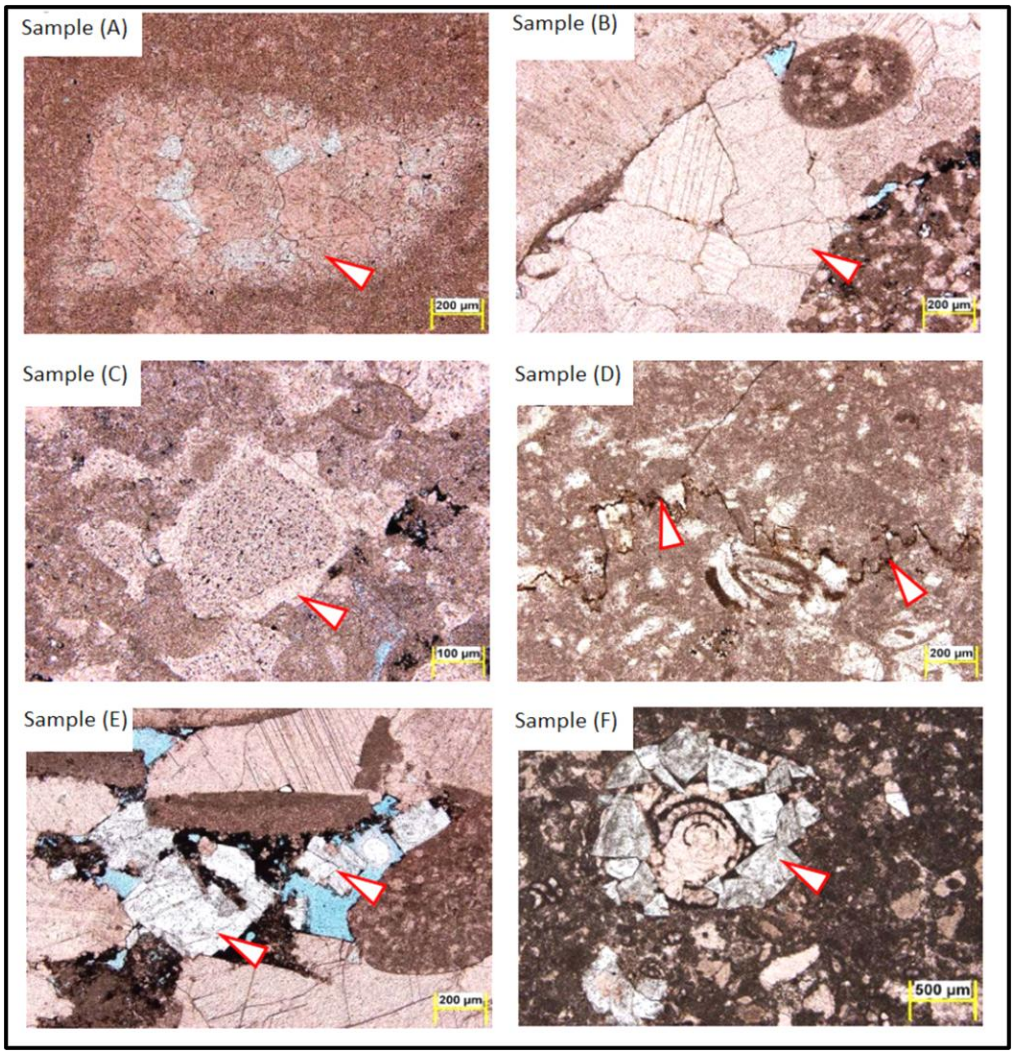

Fig. 2. Photomicrographs showing main diagenetic processes in well A: Sample A: 4593.57 m: Drusy calcite cement. Sample B: 4595.34 m: Blocky calcite cement. Sample C: 4599.45 m: Syntaxial calcite overgrowth around echinoderm plate. Sample D: 4594.24 m: Irregular stylolite with organic matter concentrated on the stylolite surface. Photo E, 4595.34 m: Euhedral dolomite rhombs partially filling Intergranular pores. Photo F, 4594.24 m: Subhedral to euhedral dolomite rhombs partially replacing foraminifera.

Materials and methods

Distinguishing the Pore Types

The Mauddud Formation's microfacies display a variety of pore types. They may be classified as primary or secondary. A number of them are listed below, as mentioned by:

a) ***Interparticle* (*Intergranular*)**: among them are the pores seen in between the grains, as shown in Fig. 3 (Sample A); the intragranular porosity is present mainly within foraminiferal tests and rudist shells, as shown in Fig. 3 (Sample B).

b) ***Moldic***: This porosity is formed after the dissolution of unstable fragments of shells such as Trocholina sp., bivalves, etc., as shown in Fig. 3 (Sample C). Interparticle pores are connected to them. However, most moldic porosity is reduced or completely plugged with calcite and/or dolomite cements.

c) ***Fracture***: Tectonic tensions within the rock cause cracks. Calcite cement can be poured into fracture pores, as shown in Fig. 3 (Sample D), or left open in another one.

d) ***Vuggy***: The breakdown of the fundamental components of limestone, including intergranular sparry calcite cement and allochems, is the cause of the vuggy pores' asymmetrical form (Al-hamdani et al., 2023). The pores are prevalent in mud- and grain-supported microfacies, cutting the matrix and the grains (Al-Dabbas et al., 2010).

There are also porosity types in the Mauddud Formation, such as channel and cavernous. These different types of pores are detected in the Mauddud Formation microfacies by categorizing pore types (Choquette and Pray, 1970).

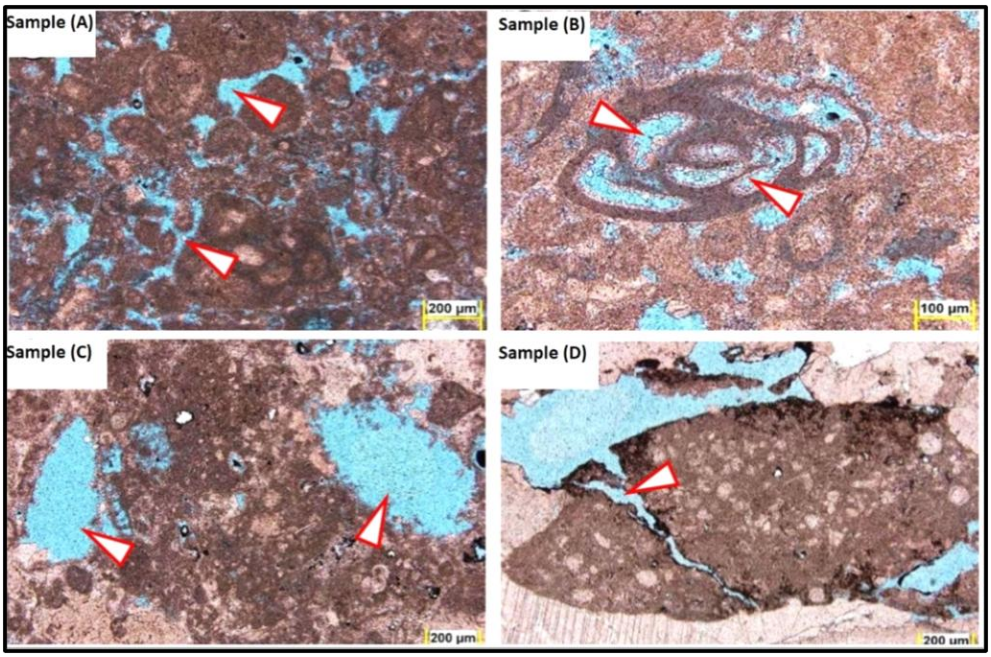

Fig. 3. Common pore types in well A: Sample. A: 4590.49 m: Intergranular porosity between fossils. Sample B: 4590.49 m: Intragranular porosity within foraminiferal tests. Sample: C: 4527.34 m: Moldic porosity through dissolution of bioclasts. Sample: D: 4595.3m: Fracture porosity due to shattering of grains.

Overburden Stress

The overburden stress, known as vertical stress, is brought on by the weight of the formations above (Zaidan et al., 2024). The overburden stress (σ_V) can be computed as follows :

$$\sigma v = \rho a * g * Z \quad \ldots\ldots\ldots 1$$

where: ρa is the average density of the underlying; g is the acceleration caused by gravity, and Z is the depth.

The vertical stress σv can be determined by integrating the densities to the depth of interest, *Z*, if the densities of the formation vary, i.e.,

$$\boldsymbol{\sigma v = \rho w * g * Zw + g \int_{zw}^{z} \rho b \, Zdz} \ldots\ldots\ldots 2$$

where: Zw is the water depth (for onshore drilling, Zw = 0); ρw is the density of seawater; and ρb is the formation bulk density as a function of depth, which can be determined from the density log.

However, density logs are usually not monitored at shallow depths. A shallow formation's bulk density can be calculated by extrapolation of the density log from the surface to the top of the log.

Pore Pressure

The total pressure effect on a certain point in a formation is the summation result of effective pressure and pore pressure (Aman et al., 2018; AlHusseini and Hamed-Allah, 2023). The effective stress will decrease with increased pore pressure, increasing the probability of failure (Zhang, 2019). Therefore, effective stress can be defined as the difference between the externally applied stress and the internal pore pressure, as established by Terzaghi (1943), or as the net stress applied to the rock skeleton:

$$\boldsymbol{\sigma` = \sigma - Pp} \ldots\ldots\ldots\ldots 3$$

where: σ` = effective stress, σ = total stress, $\boldsymbol{Pp}$ = pore pressure.

The poroelastic (α) or biot coefficient is the difference between bulk and pore volumes and explains the inter-grain connections between grains. Next, the effective stress equation is written as follows (Hettiaratchi, 1988):

$$\boldsymbol{\sigma` = \sigma - \alpha \, Pp} \ldots\ldots\ldots\ldots 4$$

The poroelastic constant has a value between zero and one; if the rocks are low-stiff, the biot coefficient (α) equals zero, and if the rocks are stiff (α=1), then the pore fluid is most effective at reducing effective stress. According to (G, 2015). The most popular approach for predicting pore pressure in the oil and gas sector is Eaton's technique (Eaton, 1975), who proposed an empirical connection to calculate pore pressure using compressional transit time data by Terzaghi (Terzaghi, 1943). According to this approach, the overburden pressure is assumed to be supported by both pore pressure and vertical effective stress, with the disequilibrium of compaction being identified as the main cause of overpressure. In this work, the non-shale zone *Pp* is computed using equation 5:

$$\boldsymbol{Pp = \sigma v - (\sigma v - Ppn) * a * \left(\frac{\Delta tn}{\Delta t}\right)^{n}} \ldots\ldots\ldots\ldots 5$$

where: Δt is the compressional transit time or slowness from the sonic log, and Δtn is the compressional transit time or slowness in shales at normal pressure. Fitting factors "a" and "n" are called the Eaton exponent and Eaton factor, respectively. The initial values are n=3 and a=1. Ppn denotes hydrostatic pore pressure.

Fracture Pressure

Fracture pressure is the point at which a rock formation cracks or breaks, potentially causing drilling fluids to leak into nearby formations. Eaton calculated the fracture pressure using the formation's Poisson's ratio and the Hubbert and Willis idea of the lowest injection pressure (Eaton, 1969; AlHusseini and Hamed-Allah, 2023):

$$\boldsymbol{Pf = \frac{v}{1-v}(\sigma v - \alpha \, Pp) + \alpha \, Pp} \ldots\ldots\ldots\ldots 6$$

where: *Pf* = the fracture pressure (psi), *v* = Poisson's ratio.

Mud Weight Window

Controlling the well mud density during drilling is crucial for ensuring safe drilling and maintaining the wellbore stability (Al-Hlaichi and Al-Mahdawi, 2023). Pore and fracture pressure are the primary variables determining the mud density value. Both static and dynamic drilling mud pressures must be lower than the fracture pressure. However, this pressure range above pore pressure is known as the mud weight window (MWW) (Charlez, 1999). It is necessary to apply mud weight within a certain range to preserve borehole stability. As shown in Fig. 4, the borehole failures can be broadly classified into four categories (Zhang, 2013):

a) Mud weight is significantly less than pore pressure, causing washouts or fluid kicks to the wellbore.
b) Mud weight being very low causes breakouts or shear failures.
c) Mud weight is too high, causing loss or lost circulation mud and resulting in tensile failure (hydraulic fractures).
d) Slide or rock failures caused by pre-existing fractures.

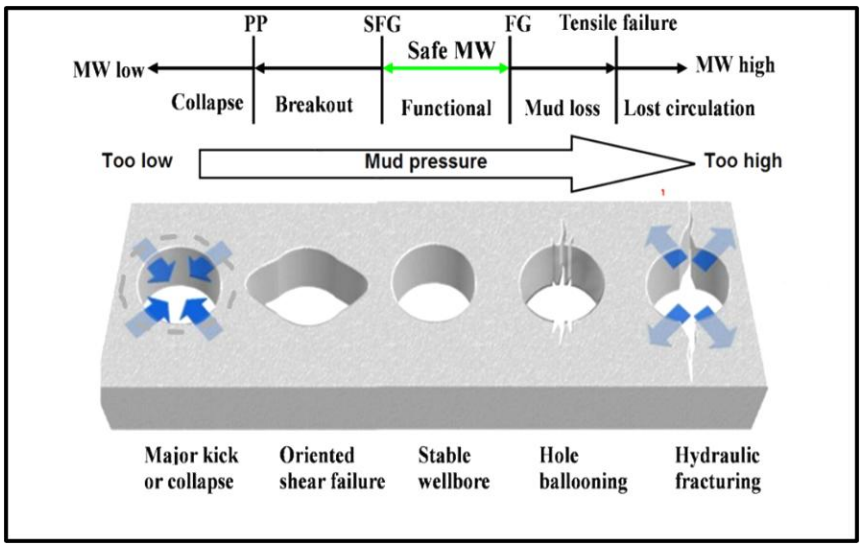

Fig. 4. Connection between borehole failures and mud pressure (mud weight, MW) (Zhang, 2013).

Microfacies Analysis of Mauddud Formation

In this study, 40 thin sections, which represent the rock core sample and cuttings, are examined, providing the information for the comprehensive study of Mauddud Formation, which was taken from four oil wells (A, B, C, and D). They are employed in the current investigation to evaluate the various depositional environments and to determine the sedimentary and stratigraphic frameworks of the sedimentary basin through the use of microfacies analysis. Five primary microfacies are found in the Mauddud sequence. These microfacies' distinctive grain types and sedimentary textures allowed for identifying the paleoenvironment; another researcher also improved this (Dunham, 1962; Flügel and Munnecke, 2010). These are:

A. Microfacies A: Wackestone-Packstone Orbitolina

Together with echinoderm and calcareous green algae, the initial microfacies contain some bioclasts from mollusks and rudists. It also contains Orbitolina sp. This could be about the deposition found in Fig. 5 (Sample A), the shallow open maritime habitat. The minute details in the Badra oil field a distributed in the middle and upper portions of the sequence under study.

B. Microfacies B: Miliolids Wackestone

These microfacies are primarily made up of pellets containing calcareous green algae, echinoderm, and orbitolinids with miliolids, in addition to bioclasts of mollusks.

The deposition in the shallow open maritime environment (Fig. 5, Sample B) is referred to as facies B. These microfacies appear in the lowest portion of the Badra oil field investigated succession.

C. Microfacies C: Bioclast, Mollusk, and Echinoderm Wackestone-Packstone

Nezzazata sp. and other bioclasts, together with mollusk and echinoderm bioclasts, are the principal constituents of this facies. These microfacies (Fig. 5, Sample C) reflect the deposition confined to semi-restricted environments. These microfacies are visible in the wells under study in the middle and upper parts of the Mauddud Formation.

D. Microfacies D: Wackestone/Bioclastic Packstone

Intraclasts, echinoderms, and fragmented rudist bioclasts are the microfacies seen in the succession, in addition to little benthic foraminifera. The slope environment is represented by microfacies (D) (Fig. 5, Sample D). The uppermost portion of the Mauddud Formation has these microfacies.

E. Microfacies E: Foraminifera/Planktonic Packstone

This less common phenomenon appears in the middle part of the Mauddud succession, composed of calcisphere and ooze with shall and marly limestones (Fig. 5, Sample E). It can be identified by high gamma ray well log reflection values and thin section diagnostics.

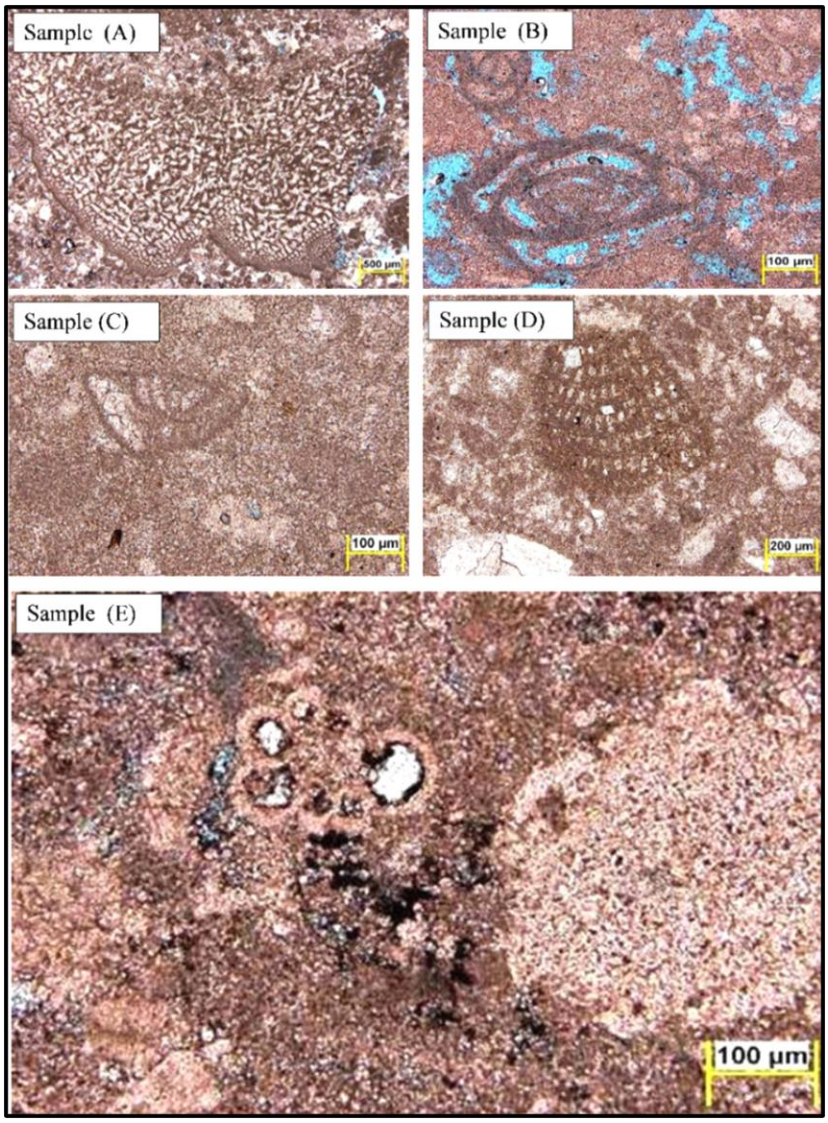

Fig. 5. Common types of Mauddud Microfacies in Badra oil felid.

Results and Discussion

Studying the pressure results of well A (Fig. 6), it seems that the values of the fracture pressure (FPRS_EATON in the third track) of the Mauddud Formation range from 9625 psi at a depth of 4485 m to 11393 psi at a depth of 4700 m. The values of fracture pressure reflect the possibility of breaking the formation; the lower value reflects an increased possibility of cracking the formation at this depth, which means the possibility of many problems, such as lost circulation, formation damage, and mud pressure decline. While high fracture pressure values reduced the possibility of mud fracturing, they increased problems such as gas/oil kicks, pipe sticking, and collapse. The overburden stress values mentioned as (SVERTACAL_EXT in the third track) range from 15346 psi at the top of the formation to 16681 psi at the bottom. Studying the results of pore pressure (PPRS_EATON_S in the third track) explains that it ranges from 8000 psi at 4485m to 10027 psi at 4700 m. The obtained pore pressure values of the current study are close to the measured values mentioned in previous research literature (Kareem, 2020). The high pore pressure calculated at different levels of the Mauddud Formation is mainly caused by compaction. Compaction leads to reduced porosity and volume of rocks resulting from overburdened sediment thickness. The formation structure appears to be a narrow NW-SE trending anticline accompanied by long normal faults. The area contains two NW-SE trending sets of low amplitude buried anticlines associated with longitudinal faults and a transverse EW trend. High formation pressure results from the Foothill zone, part of an unstable shelf (Kareem, 2020).

The suggested value of this well's Mud Weight Window (MWW), which indicates the difference between pore pressure and fracture pressure values, is about (2.7-2.9 ppg) and is considered a safe value for drilling the interested formations.

Analyzing the results of different pressures across the field provides an important estimation of the real situation of the anticline structure of the reservoir. This can be done by analyzing the results of other wells in different locations over the field. Pressure analysis of well B (Fig. 7) shows that the values of the fracture pressure (FPRS_EATON in the third track) range from 10240 psi at a depth of 4456 m to 11525 psi at a depth of 4621 m. The values of overburden stress (SVERTACAL_AVG in the third track) range from 14580 psi at 4454 to 15680 psi at 4763m. The pore pressure results (PPRS_EATON_S in the third track) show that they range from 8063 psi at 4456m to 9703 psi at 4621m. The estimated Mud Weight Window for this well is about (2.7-3.4 ppg).

On the other hand, the results of well C (Fig. 8) show that the values of the fracture pressure (FPRS_EATON in the third track) range from 10561 psi at a depth of 4470 m to 12082 psi at a depth of 4606 m. At the same time, the values of overburden stress (SVERTACAL_EXT in the third track) range from 15788 psi at 4470 to 17050 psi at 4824 m. Studying pore pressure results (PPRS_EATON_S in the third track) explains that the pressure ranges from 7947 psi at 4470 m to 9986 psi at 4606 m. The estimated Mud Weight Window for this well is about (2.3-2.8 ppg).

In the fourth well D (Fig. 9), it is found that the values of the fracture pressure (FPRS_EATON in the third track) range from 10420 psi at a depth of 4539 m to 12467 psi at a depth of 4919 m. While the values of overburden stress (SVERTACAL_EXT in the third track) range from 15122 psi at 4539 to 16498 psi at 4921 m. Studying pore pressure results (PPRS_EATON_S in the third track) shows that the pressure ranges from 8070 psi at 4539 m to 10457 psi at 4919 m. The estimated Mud Weight Window for this well is about (2.4-3.1 ppg).

A comprehensive study of the four wells shows that the lowest value for the fracture pressure is recorded in well A, which means that the well is the most exposed to the fracturing problem. The σ_V values are almost high, and the pressure gradient value is more than 1 psi/ft,

which causes the problem of instability of layers and thus stuck pipe in most wells. The largest value of σ_V is observed in well C. Accordingly, this well is the most exposed to this problem.

If the value of the pore pressure is greater than the fracture pressure in specific areas of the Mauddud Formation, this will lead to a kicking problem, and therefore, the pressure of the drilling mud in those areas must be increased. The highest value of pore pressure recorded in the well D (Fig. 9) is 10457 psi at a depth of 4919 m. This explains the relative difference between the measured mud density (MW_meas in the fourth track) and the equivalent calculated mud density (PPMW_EATON_S).

Finally, the widest MWW is estimated in well B, located at the crest of the anticline structure of the field, and is considered the best well relative to safety drilling operations. In contrast, the safe mud weight window becomes narrower and more dangerous for other wells located near the edge of the anticline structure of the fields.

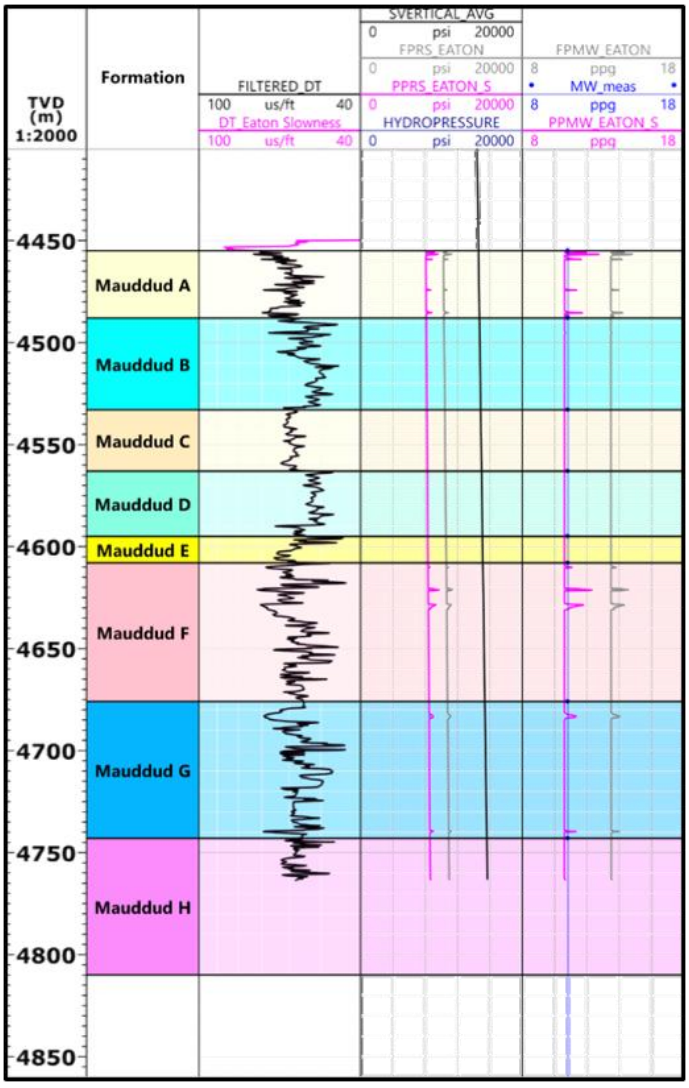

Fig. 6. Pore and fracture pressures in well A.

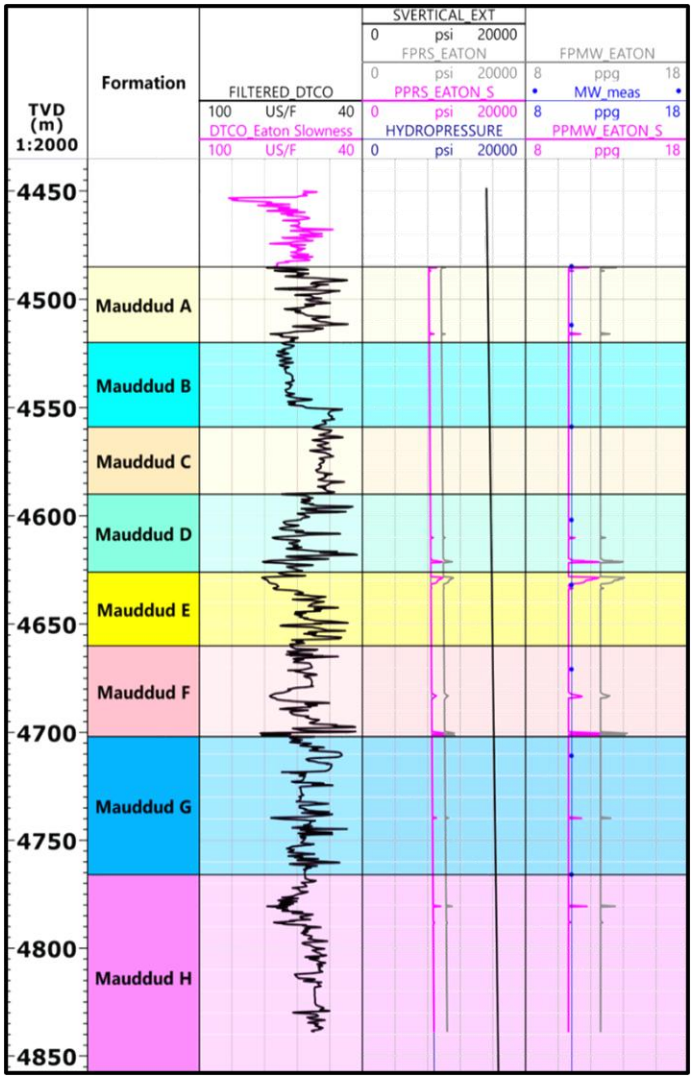

Fig. 7. Pore and fracture pressures in well B.

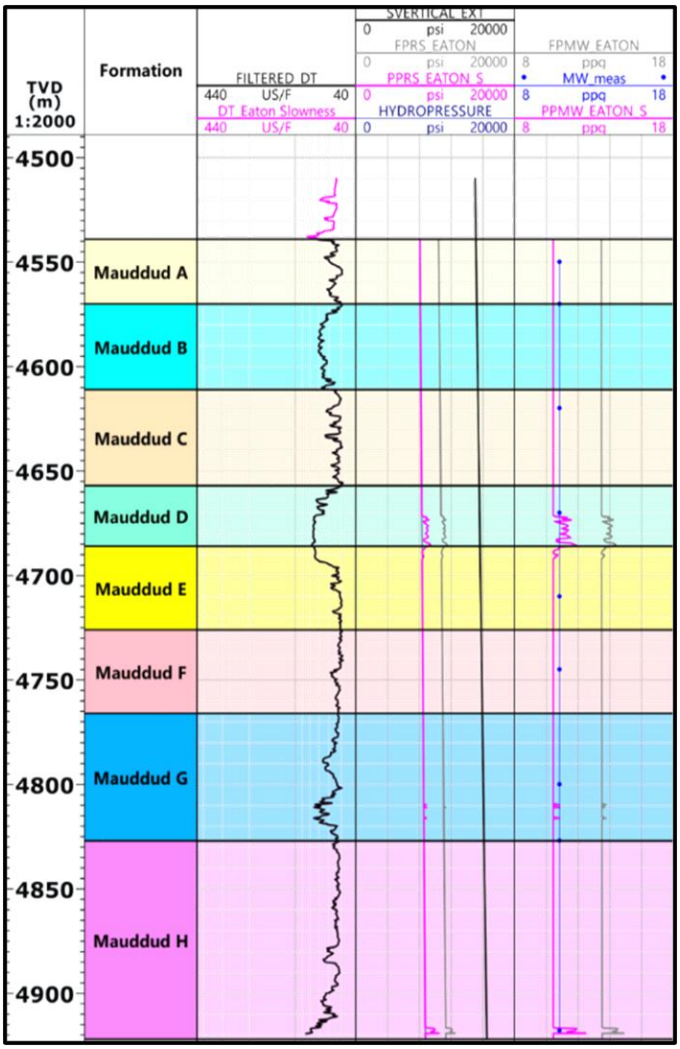

Fig. 8. Pore and fracture pressures in well A.

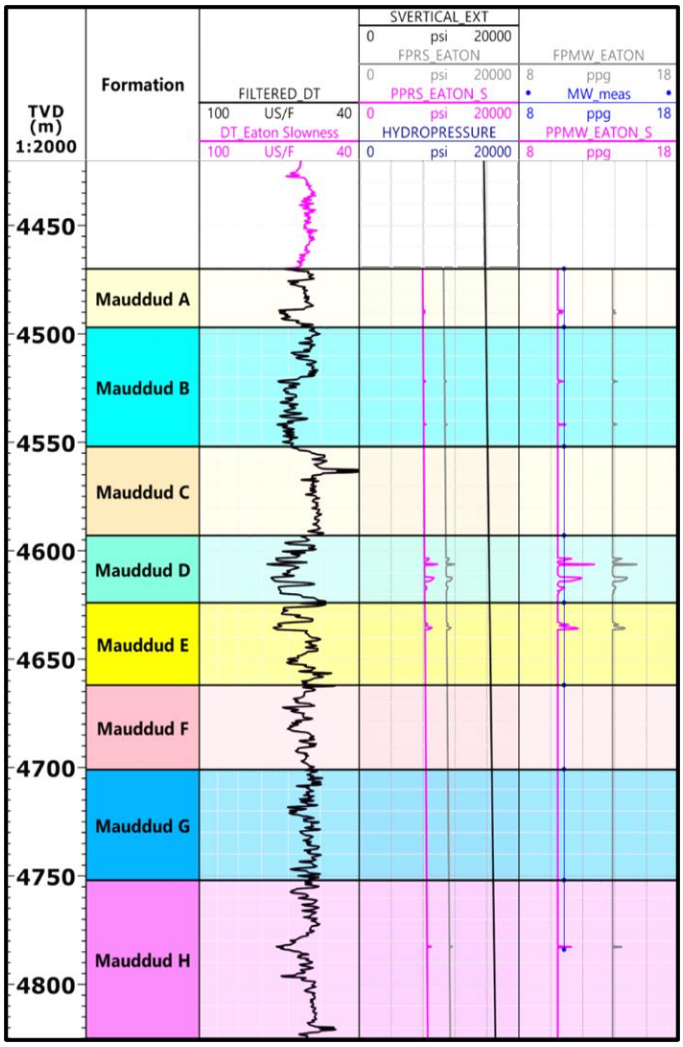

Fig. 9. Pore and fracture pressures in well D.

Conclusions

This section highlights the main investigation from the estimated results of different pressure types of the Badra oil field interval Mauddud Formation. It is concluded that the prediction of mud weight along the studied formation shows that the value of a safe mud weight window must range from 2.3 to 3.4 ppg and becomes narrower and more dangerous when the wells cross the edge of the anticline structure of the reservoir. This result is acceptable since the higher difference between the maximum and minimum horizontal stress values is concentrated at the edge of the geological structure. In other words, drilling the wells near the crest of the studied formation is recommended to avoid the narrow mud weight window expected in the formation's structural edge.

References

Aadnoy, B.S. and Ong, S., 2003. Introduction to the special issue on borehole stability. Journal of Petroleum Science and Engineering, Vol. 38, No. 3, pp.79–82. https://doi.org/10.1016/S0920-4105(03)00022-6

Aadnoy, B.S. and Looyeh, R., 2011. Petroleum Rock Mechanics: Drilling Operations and Well Design, 1st Edition. In Oxford: Gulf Professional Publishing. https://www.scribd.com/book/413520471/Petroleum-Rock-Mechanics-Drilling-Operations-and-Well-Design

Al-Dabbas, M.A., Jassim, J.A. and Qaradaghi, A.I., 2010. Sedimentological and depositional environment studies of the Mauddud formation, central and southern Iraq. Arabian Journal of Geosciences, 5(2), pp. 297–312. https://doi.org/10.1007/s12517-010-0256-5

Al-hamdani, D.M., Abdullah, M.H., Al-Hameedy, R. and Al Hamdani, S.A., 2023. Porosity Type Determination Using the Velocity Deviation Technique for The Sheikh Allas Formation in The Kirkuk Oil Field, Northeastern Iraq. Iraqi National Journal of Earth Science (INJES), 23(2), pp. 20–36. https://doi.org/10.33899/earth.2023.139106.1059

Al-Hlaichi, S.K. and Al-Mahdawi, F.H.M., 2023. Drilling Optimization by Using High Drilling Techniques: A Review. AIP Conference Proceedings, 2839(1), pp. 53–64. https://doi.org/10.1063/5.0167961

AlHusseini, A.K. and Hamed-Allah, S.M., 2023. Estimation Pore and Fracture Pressure Based on Log Data; Case Study: Mishrif Formation/Buzurgan Oilfield at Iraq. Iraqi Journal of Chemical and Petroleum Engineering, 24(1), pp. 65–78. https://doi.org/10.31699/ijcpe.2023.1.8

Aman, M., Espinoza, D.N., Ilgen, A.G., Major, J.R., Eichhubl, P. and Dewers, T.A., 2018. CO2-induced chemo-mechanical alteration in reservoir rocks assessed via batch reaction experiments and scratch testing. Greenhouse Gases: Science and Technology, 8(1), pp. 133–149. https://doi.org/https://doi.org/10.1002/ghg.1726

Bandara, M.K. and Al-Ameri, N.J., 2024. Wellbore Instability Analysis to Determine the Safe Mud Weight Window for Deep Well, Halfaya Oilfield. Iraqi Geological Journal, 57(1D), pp. 153–173. https://doi.org/10.46717/igj.57.1D.13ms-2024-4-23

Charlez, P.A., 1999. The concept of mud weight window applied to complex drilling. SPE Annual Technical Conference and Exhibition, SPE-56758. https://doi.org/https://doi.org/10.2118/56758-MS

Chen, S., 2017. Petroleum Production Engineering. Springer Handbook of Petroleum Technology, pp. 501–516. https://doi.org/https://link.springer.com/chapter/10.1007/978-3-319-49347-3_14

Choquette, P.W. and Pray, L.C., 1970. Geologic nomenclature and classification of porosity in sedimentary carbonates. AAPG Bulletin, 54(2), pp. 207–250. https://doi.org/10.1306/5D25C98B-16C1-11D7-8645000102C1865D

Croizé, D., 2010. Mechanical and chemical compaction of carbonates: an experimental study. University of Oslo, Norway. https://doi.org/https://www.duo.uio.no/bitstream/handle/10852/12547/2/PhD-Croize.pdf

Cross, N., Goodall, I., Hollis, C., Burchette, T., Al-Ajmi, H.Z.D., Johnson, I.G., Mukherjee, R., Simmons, M. and Davies, R., 2010. Reservoir description of a mid-Cretaceous siliciclastic-carbonate ramp reservoir: Mauddud Formation in the Raudhatain and Sabiriyah fields, North Kuwait. GeoArabia, 15(2), pp. 17–50. https://doi.org/https://archives.datapages.com/data/specpubs/carbona2/data/a038/a038/0001/0100/0108.html

Dunham, R.J., 1962. Classification of carbonate rocks according to depositional textures. https://onepetro.org/JPT/article-abstract/21/10/1353/164490

Eaton, B.A., 1969. Fracture gradient prediction and its application in oilfield operations. Journal of Petroleum Technology, 21(10), pp. 1353–1360. https://doi.org/onepetro.org/JPT/article-abstract/21/10/1353/164490

Eaton, B.A., 1975. The equation for geopressure prediction from well logs. SPE Annual Technical Conference and Exhibition, SPE--5544. https://doi.org/10.2118/5544-MS

Enos, P., 1988. Evolution of pore space in the Poza Rica trend (Mid-Cretaceous), Mexico. Sedimentology, 35(2), pp. 287–325. https://doi.org/10.1111/j.1365-3091.1988.tb00950.x

Faisal, M.J. and Mahdi, T.A., 2020a. Diagenetic processes overprint and pore types of Mauddud formation, Badra oil field, Central Iraq. Iraqi Journal of Science, 61(6), pp. 1353–1361. https://doi.org/10.24996/ijs.2020.61.6.13

Faisal, M.J. and Mahdi, T.A., 2020b. Geological model of Mauddud Formation in Badra Oilfield. The Iraqi Geological Journal, pp. 58–67. https://doi.org/10.46717/igj.53.1a.R4.2020.01.28

Flügel, E., 2012. Microfacies analysis of limestones. Springer Science and Business Media. https://doi.org/10.1007/978-3-642-68423-4

Flügel, E. and Munnecke, A., 2010. Microfacies of carbonate rocks: analysis, interpretation and application, Vol. 976, Springer. https://doi.org/10.1007/978-3-662-08726-8

Folk, R.L., 1965. Some aspects of recrystallization in ancient limestones. https://onepetro.org/ARMAUSRMS/proceedings-abstract/ARMA69/All-ARMA69/130984abstract/ARMA69/All-ARMA69/130984

G, Z.U., 2015. An overview of pore pressure prediction using seismicallyderived velocities. Journal of Geology and Mining Research, 7(4), pp. 31–40. https://doi.org/10.5897/JGMR15.0218

Ghafor, I., Fatah, A. and Khafaf, A.A.L., 2023. Biostratigraphy and Microfacies of the Mauddud Formation (Late Albian–Early Cenomanian) in Musaiyib Well No. 1, Central Iraq. Iraqi Bulletin of Geology and Mining, 19(2), pp. 37–56. https://doi.org/https://doi.org/10.59150/ibgm1902a03

Haimson, B. and Fairhurst, C., 1969. In-situ stress determination at great depth by meansing hydraulic fracturing. ARMA US Rock Mechanics/Geomechanics Symposium, ARMA-69. https://doi.org/10.1016/0167-1987(88)90005-0

Hettiaratchi, D., 1988. Theoretical soil mechanics and implement design. Soil and Tillage Research, 11(3–4), pp. 325–347. https://doi.org/10.1306/2F918A63-16CE-11D7-8645000102C1865D

Jassim, S.Z. and Goff, J.C., 2006. Geology of Iraq. DOLIN, sro, distributed by the Geological Society of London. https://doi.org/https://www.sciencedirect.com/science/article/pii/0167198788900050

Kareem, K.A., 2020. Optimization of Water Injection for Badra Oil Field. 53(1), pp. 13–28. https://doi.org/10.46717/igj.53.1B.2Rz-2020-03-02

Longman, M.W., 1980. Carbonate diagenetic textures from nearsurface diagenetic environments. AAPG Bulletin, 64(4), pp. 461–487. https://doi.org/https://books.google.com/books

Najibi, A.R., Ghafoori, M., Lashkaripour, G.R. and Asef, M.R., 2017. Reservoir geomechanical modeling: In-situ stress, pore pressure, and mud design. Journal of Petroleum Science and Engineering, 151, pp. 31-39.

Rasouli, V., Pallikathekathil, Z.J. and Mawuli, E., 2011. The influence of perturbed stresses near faults on drilling strategy: a case study in Blacktip field, North Australia. Journal of Petroleum Science and Engineering, 76(1–2), pp. 37–50. https://doi.org/10.1306/04220301111

Sadooni, F.N. and Alsharhan, A.S., 2003. Stratigraphy, microfacies, and petroleum potential of the Mauddud Formation (Albian–Cenomanian) in the Arabian Gulf basin. AAPG Bulletin, 87(10), pp. 1653–1680. https://doi.org/10.1306/04220301111

Scholle, P.A. and Ulmer-Scholle, D., 2005. A Color Guide to the Petrography of Carbonate Rocks: Grains, Textures, Porosity, Diagenesis. AAPG Memoir, 77, 486 P. https://doi.org/10.1306/M77973

Terzaghi, K., 1943. Theoretical soil mechanics. https://doi.org/libarch.nmu.org.ua/bitstream/handle/GenofondUA/19513/fe8e4061e420c7a5c38e39e9774911c0.pdf?sequence=1

Kareem, K.A., 2020. Optimization of water injection for Badra oil field Wasit, southern Iraq. The Iraqi Geological Journal, Vol. 53, No. 1B, pp. 13-28. https://doi.org/10.46717/igj.53.1B.2Rz-2020-03-02

Zaidan, A.F., Hadi, F.A. and Klempa, M., 2024. Investigation of Wellbore Instability in Southern Rumaila Oil Field. Iraqi Journal of Chemical and Petroleum Engineering, 25(2), pp. 17–31. https://doi.org/10.31699/ijcpe.2024.2.2

Zhang, J., 2013. Borehole stability analysis accounting for anisotropies in drilling to weak bedding planes. International Journal of Rock Mechanics and Mining Sciences, 60, pp. 160–170. https://doi.org/10.1016/j.ijrmms.2012.12.025

Zhang, J.J., 2019. Applied Petroleum Geomechanics. In Loess and Loess Geohazards in China. https://doi.org/10.1201/9781315177281-4